

Nonlinear Local Lyapunov Exponent and Quantification of Local Predictability *

DING Rui-Qiang(丁瑞强)¹, LI Jian-Ping(李建平)^{1**}, HA Kyung-Ja²

¹State Key Laboratory of Numerical Modeling for Atmospheric Sciences and Geophysical Fluid Dynamics (LASG),
Institute of Atmospheric Physics, Chinese Academy of Sciences, Beijing 100029

²Division of Earth Environmental System, Pusan National University, Busan 609-735, Korea

(Received 3 December 2007)

Nonlinear local Lyapunov exponent (NLLE) is applied to quantitatively determine the local predictability limit of chaotic systems. As an example, we find that the local predictability limit of Henon attractor varies considerably with time, and some underlying phase-spatial structure does not appear. The local predictability limit of initially adjacent points in phase space may be completely different. This will cause difficulties in making the long-time analogue forecast.

PACS: 95.10.Fh, 92.60.Wc

Lyapunov exponents give a measure of the long-term average exponential rate of divergence or convergence of initially adjacent phase space trajectories on an attractor. When at least one Lyapunov exponent is positive, the attractor is chaotic and initially nearby trajectories diverge exponentially, on average. For these attractors, the largest Lyapunov exponent defines an average predictability time scale. An increase of magnitude of the largest Lyapunov exponent implies a decrease of predictability time scale.^[1] According to Oseledec's multiplicative ergodic theorem,^[2] Lyapunov exponents are almost constant everywhere on an attractor, thus describing the global characteristics of the attractor. However, the divergence rate of nearby trajectories is not all the same on all parts of a chaotic attractor. Often we could be interested in the local predictability on the chaotic attractor, and its estimation has been an important subject in the predictability studies.

Temporal variation of predictability was originally investigated by Lorenz^[3] with a low-order (28 variables) spectral model. He examined the amplification rate of root mean square error during a prescribed time interval (hereafter inferred to as the Lorenz index), and found that growth of small perturbations shows large variability depending upon the state of the reference solution. Afterwards Nese^[4] calculated local divergence rates for the Lorenz attractor and investigated both the temporal and phase-spatial variations in predictability. The results show that predictability varies considerably with time, but there is phase-spatial organization to the variability. Mukougawa *et al.*^[5] adopted the Lorenz index to investigate the properties of the local predictability on the Lorenz attractor. They pointed out the role of the unstable stationary point in determining the fine phase-spatial organization of the local predictability on the Lorenz attractor. Recently, local or finite-time Lyapunov exponents have been defined for a prescribed

finite-time interval to study the local dynamics on an attractor.^[6-8]

Compared with the global Lyapunov exponent, the Lorenz index, local or finite-time Lyapunov exponents characterize the nonuniform spatial organization and provide information on the variation of predictability on chaotic attractors. However, these quantities are established on the basis of the fact that the initial perturbations are sufficiently small such that the evolution of them can be governed approximately by the tangent linear model (TLM), which essentially belongs to linear error dynamics. Clearly, although two initially nearby trajectories on a chaotic attractor remain nearby in a short time, they eventually diverge. Therefore, the Lorenz index, local or finite-time Lyapunov exponents are only applicable to study the local predictability under conditions of sufficiently small perturbation and short time intervals. In the situations of finite perturbation or long time intervals, these quantities are not effective anymore.^[9,10]

In view of the limitations of the quantities mentioned above, it is necessary to propose a new approach based on nonlinear error growth dynamics for quantifying the local predictability of chaotic systems. Therefore, we introduce a definition of the nonlinear local Lyapunov exponent (NLLE) recently.^[11,12] The NLLE measures the growth rate of initial errors of nonlinear dynamical models without linearizing the governing equations, which is a nonlinear generalization to the existing local or finite-time Lyapunov exponents. The NLLE and its derivatives have been used to quantitatively determine the global average predictability limit of chaotic systems.^[12,13] In this Letter, applications of the NLLE in investigating the local predictability of chaotic systems are introduced. We take the Henon map as the example to investigate quantitatively both the temporal and phase-spatial variability of local predictability limit on a chaotic attractor.

*Supported by the National Key Basic Research Programme of China under Grant No 2006CB403600, and the National Natural Science Foundation of China under Grant Nos 40675046 and 40325015.

** Email: ljp@lasg.iap.ac.cn

© 2008 Chinese Physical Society and IOP Publishing Ltd

Let us to consider an n -dimensional continuous-time dynamical system, which is defined by a set of nonlinear ordinary differential equations:

$$\frac{d}{dt}\mathbf{x}(t) = \mathbf{F}[\mathbf{x}(t)], \quad (1)$$

where $\mathbf{x}(t) = (x_1(t), x_2(t), \dots, x_n(t))^T$ and the superscript T indicates transpose. A solution of (1), $\mathbf{x}(t)$ will be called a reference solution.

Let $\boldsymbol{\delta}(t_0)$ be a small perturbation superimposed on $\mathbf{x}(t_0)$ at the initial time $t = t_0$. Without the tangent linear approximation, the evolution of the small perturbation $\boldsymbol{\delta}(t)$ is given by

$$\frac{d}{dt}\boldsymbol{\delta}(t) = \mathbf{J}(\mathbf{x}(t))\boldsymbol{\delta}(t) + \mathbf{G}(\mathbf{x}(t), \boldsymbol{\delta}(t)), \quad (2)$$

where $\mathbf{J}(\mathbf{x}(t))\boldsymbol{\delta}(t)$ are the tangent linear terms, $\mathbf{J}(\mathbf{x}(t))$ denotes the $n \times n$ Jacobian matrix: $J_{ij} = \partial F_i / \partial x_j$, and $\mathbf{G}(\mathbf{x}(t), \boldsymbol{\delta}(t))$ are the high order nonlinear terms of the perturbations $\boldsymbol{\delta}$. The solutions (2) can be obtained by numerically integrating it along the reference solution from $t = t_0$ to $t_0 + \tau$:

$$\boldsymbol{\delta}(t_0 + \tau) = \boldsymbol{\eta}(\mathbf{x}(t_0), \boldsymbol{\delta}(t_0), \tau)\boldsymbol{\delta}(t_0), \quad (3)$$

where $\boldsymbol{\eta}(\mathbf{x}(t_0), \boldsymbol{\delta}(t_0), \tau)$ is defined as the nonlinear propagator, which, as described by Eq. (3), propagates the initial perturbation forward to the perturbation at $t = t_0 + \tau$. The nonlinear propagator $\boldsymbol{\eta}(\mathbf{x}(t_0), \boldsymbol{\delta}(t_0), \tau)$ is different from the linear propagator $\mathbf{M}(\mathbf{x}(t_0), \tau)$,^[6,7] which is within the framework of infinitesimal initial perturbations and does not depend on the initial perturbation $\boldsymbol{\delta}(t_0)$. Then the nonlinear local Lyapunov exponent (NLLE) is defined as

$$\lambda(\mathbf{x}(t_0), \boldsymbol{\delta}(t_0), \tau) = \frac{1}{\tau} \ln \frac{\|\boldsymbol{\delta}(t_0 + \tau)\|}{\|\boldsymbol{\delta}(t_0)\|}, \quad (4)$$

where $\lambda(\mathbf{x}(t_0), \boldsymbol{\delta}(t_0), \tau)$ depends in general on the initial state in phase space $\mathbf{x}(t_0)$, the initial perturbation $\boldsymbol{\delta}(t_0)$, and time τ . In the double limit as $\|\boldsymbol{\delta}(t_0)\| \rightarrow 0$ and $\tau \rightarrow \infty$, the NLLE converges to the largest global Lyapunov exponent λ_1 .^[1] For the specified initial perturbation $\boldsymbol{\delta}(t_0)$, if we take the ensemble average of the NLLE over a large number of initial states, the global average error growth of chaotic systems can be studied.^[11–13] However, for the specified initial state $\mathbf{x}(t_0)$, if we take the local ensemble average of the NLLE over a large number of random initial perturbations with the same magnitude and different random directions, the local average error growth of chaotic systems can be investigated.

Assuming that all initial perturbations with the amplitude ε and random directions are on an n -dimensional spherical surface centered at an initial point $\mathbf{x}(t_0)$,

$$\boldsymbol{\delta}^T(t_0)\boldsymbol{\delta}(t_0) = \varepsilon^2. \quad (5)$$

The local ensemble mean of the NLLE over a large number of random initial perturbations is given by

$$\bar{\lambda}(\mathbf{x}(t_0), \tau) = \langle \lambda(\mathbf{x}(t_0), \boldsymbol{\delta}(t_0), \tau) \rangle_N, \quad (6)$$

where $\langle \rangle_N$ denotes the local ensemble average of samples of large enough size N ($N \rightarrow \infty$). Here $\bar{\lambda}(\mathbf{x}(t_0), \tau)$ characterizes the average growth rate of random perturbations superimposed on $\mathbf{x}(t_0)$ within a finite time τ . For a fixed time τ , $\bar{\lambda}(\mathbf{x}(t_0), \tau)$ varies with different $\mathbf{x}(t_0)$ and reflects the local error growth dynamics of the attractor. The mean local relative growth of initial error (LRGIE) can be obtained by

$$\bar{E}(\mathbf{x}(t_0), \tau) = \exp(\bar{\lambda}(\mathbf{x}(t_0), \tau)\tau). \quad (7)$$

For a certain initial state $\mathbf{x}(t_0)$, $\bar{E}(\mathbf{x}(t_0), \tau)$ initially increases with time τ and finally reaches the states of nonlinear stochastic fluctuation, which means that error growth reaches saturation with a constant average value. At that moment almost all information on initial states is lost and the prediction becomes meaningless. If the local predictability limit is defined as the time at which error reaches the average value of nonlinear stochastic fluctuation states, the predictability limit of the system at $\mathbf{x}(t_0)$ can be quantitatively determined. The NLLE and its derivatives enable us to quantitatively determine the local predictability limit, which is a major advantage of the new approach.

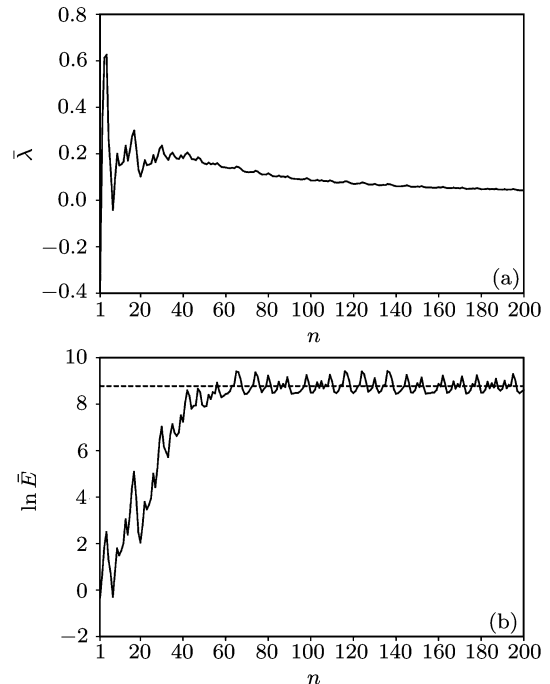


Fig. 1. For the initial state on the Henon attractor $\mathbf{x}_1(0.197, 0.195)$, the mean NLLE $\bar{\lambda}(\mathbf{x}(t_0), n)$ (a) and the logarithm of $\bar{E}(\mathbf{x}(t_0), n)$ (b) with $\varepsilon=10^{-4}$ as a function of time step n . The average value of the nonlinear stochastic fluctuation states of the mean RLGIE is indicated by the constant dashed line in (b).

The example is given by the Henon map,^[14]

$$\begin{cases} x_{n+1} = 1 - ax_n^2 + y_n, \\ y_{n+1} = bx_n, \end{cases} \quad (8)$$

where $a = 1.4$ and $b = 0.3$. For two different initial states on the Henon attractor $\mathbf{x}_1 (0.197, 0.195)$ and $\mathbf{x}_2 (-0.96, 0.36)$, Figures 1 and 2 show their variations of $\bar{\lambda}(\mathbf{x}(t_0), n)$ and the logarithm of $\bar{E}(\mathbf{x}(t_0), n)$ with $\varepsilon = 10^{-4}$ as a function of time n (equivalent to the time τ in Eqs. (6) and (7)), respectively. Here $\bar{\lambda}(\mathbf{x}(t_0), n)$ is obtained by averaging the NLLE $\lambda(\mathbf{x}(t_0), \delta(t_0), n)$ over 1×10^5 random initial perturbations. It can be seen that $\bar{\lambda}(\mathbf{x}_1(t_0), n)$ initially oscillates between positive and negative values, then shows fluctuations around a small positive value and finally decreases gradually and approaches zero as n increases (Fig. 1(a)). Correspondingly, after the zigzag growth process, $\bar{E}(\mathbf{x}_1(t_0), n)$ finally stops growing and enters the nonlinear stochastic fluctuation states with the constant average value (Fig. 1(b)). If the local predictability limit is defined as the time at which error reaches the average value of nonlinear stochastic fluctuation states, the predictability limit at \mathbf{x}_1 with $\varepsilon = 10^{-4}$ is $T_P = 55$.

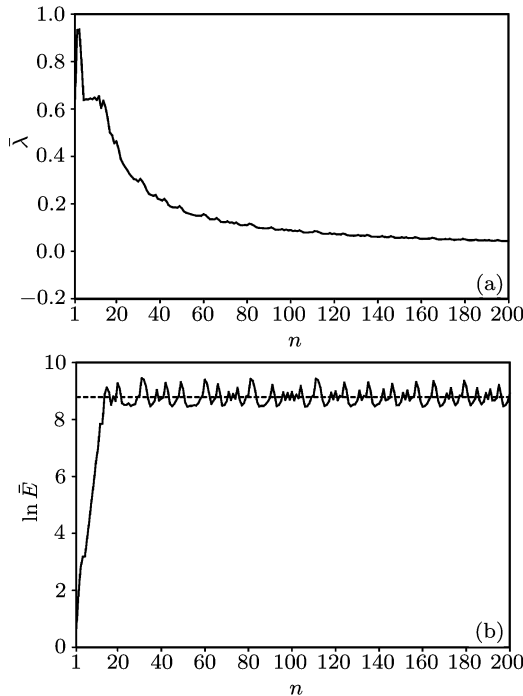


Fig. 2. The same as Fig. 1 but for the other initial state on the Henon attractor $\mathbf{x}_2 (-0.96, 0.36)$.

Compared with \mathbf{x}_1 , the predictability at \mathbf{x}_2 is very low. Then $\bar{\lambda}(\mathbf{x}_2(t_0), n)$ initially appears a large positive value, and finally decreases gradually and approaches zero as n increases (Fig. 2(a)). Correspondingly, $\bar{E}(\mathbf{x}_2(t_0), n)$ initially grows so quickly that it stops growing and enters the nonlinear stochastic fluctuation states in a very short time (Fig. 2(b)). According to the definition, the predictability limit at \mathbf{x}_2 can

be obtained to be $T_P = 14$, which is much smaller than that at \mathbf{x}_1 . The results indicate that the NLLE and its derivatives can characterize well the finite-time error growth and local predictability on the attractor.

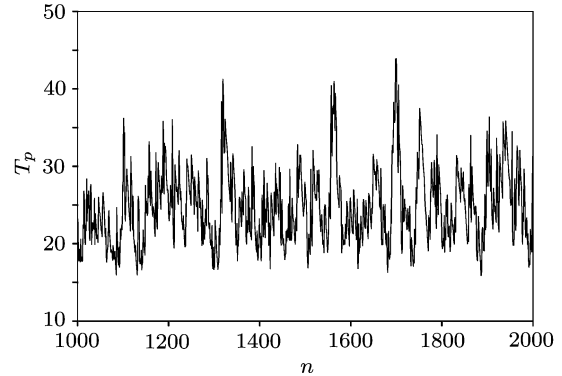


Fig. 3. Local predictability limit on the Henon attractor as a function of initial states $\mathbf{x}_n (n = 1000 \sim 2000)$.

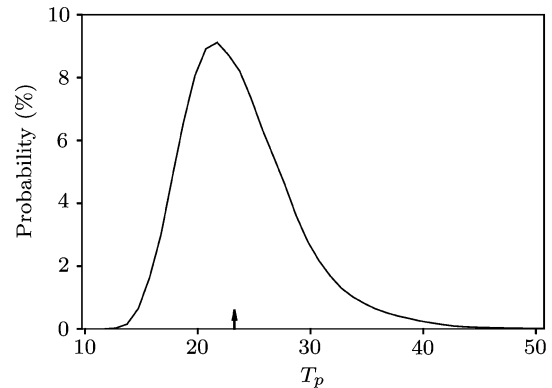


Fig. 4. Estimated probability density of the local predictability limit on the Henon attractor.

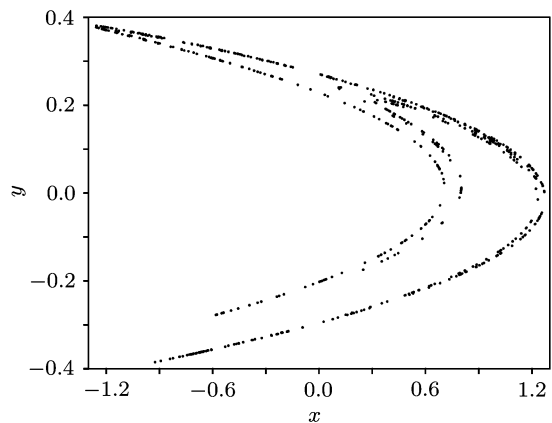


Fig. 5. Distribution of the local predictability limit on the Henon attractor. It is indicated by closed circles if the local predictability limit of a location in phase space is larger than 35.

Figure 3 shows the variation of the local predictability limit as a function of initial states \mathbf{x}_n (i.e., phase space position) for a portion of a typical trajectory on the Henon attractor. It can be seen that the

local predictability limit varies widely on the Henon attractor. Integrating for 3×10^4 time steps, we find a maximum value of the local predictability limit exceeding 55, while the minimum value is approximately 13. Figure 4 shows the probability density curve of the local predictability limit on the Henon attractor. The peak in the probability density curve occurs at $T_P = 22$. The very large or small values of the local predictability limit both occur with a low probability. The average value \bar{T}_P of the local predictability limit on the Henon attractor is shown with an arrow in Fig. 4. We find that the cumulative probability of $T_P \leq \bar{T}_P$ is approximately equal to 0.54.

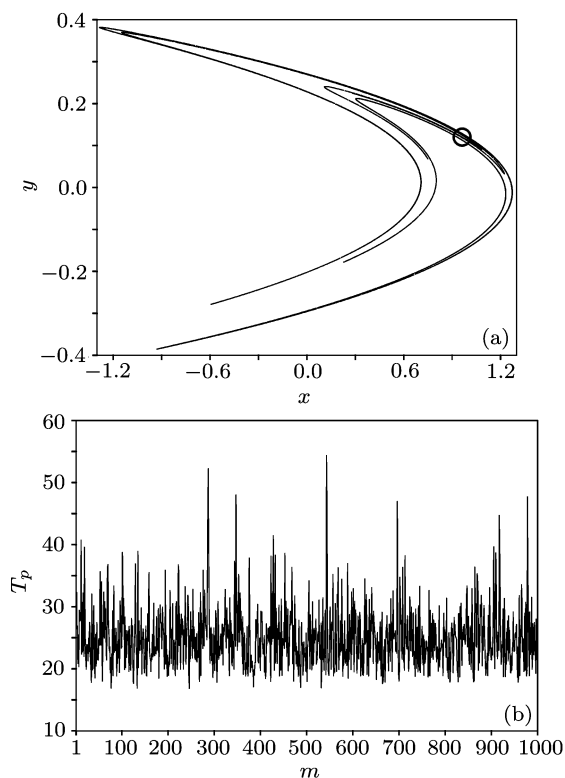


Fig. 6. A very small region on the Henon attractor is chosen by a circle (a), and the variations of the local predictability limit of the first 1000 points with the order of the typical trajectory entering the small region (b).

For a chaotic attractor, the local predictability limit actually gives a measure of long time-scale local predictability on the attractor. It is different from the local divergence rates or local Lyapunov exponent, which are restricted to conditions of sufficiently small perturbations and only applicable to reflect the short time-scale local predictability. Therefore, the distribution of the local predictability limit does not appear some regions of underlying high predictability or low predictability in phase space. The locations of high predictability are distributed everywhere on the Henon attractor (Fig. 5). It also holds true for the locations of low predictability on the Henon attractor (not shown).

We choose a very small region on the Henon at-

tractor (Fig. 6(a)) and sort according to the order of the typical trajectory entering the small region. The first entering point is recorded as $m = 1$, the second entering point is recorded as $m = 2$, and so on. Figure 6(b) shows the variation of the local predictability limit of the first 1000 points with the order of the typical trajectory entering the small region. It can be seen that the local predictability limit of nearby locations in the small region shows big differences. The variation range of the local predictability limit in the small region almost covers the one on the whole attractor. This implies that the local predictability limit of initially adjacent points might be completely different. For this reason, the capability that makes the long-range analogue forecast^[15,16] is greatly reduced.

In summary, with the nonlinear local Lyapunov exponent (NLLE) and its derivatives, both global average predictability limit and local predictability limit of a chaotic attractor can be quantitatively determined. We focus on the applications of the NLLE in investigating the local predictability of chaotic systems. Local predictability limit gives a measure of long time-scale local predictability on the attractor. As an example, the local predictability limit of Henon attractor is calculated. It is found that the local predictability limit on the Henon attractor varies considerably with time, and does not appear some underlying phase-spatial structure. The local predictability limit of initially adjacent points in phase space might be completely different. This will cause difficulties of making the long-time analogue forecast. Temporal variation of the atmospheric predictability is noticeable in medium and extended ranges.^[17,18] The prediction of forecast skill is an important subject in medium-range weather forecasts. By applying the NLLE to the numerical weather forecasts, to providing an estimate of the skill of a particular forecast, a priori will be a further subject of future research.

References

- [1] Eckmann J P and Ruelle D 1985 *Rev. Mod. Phys.* **57** 617
- [2] Oseledec V I 1968 *Trans. Moscow Math. Soc.* **19** 197
- [3] Lorenz E N 1965 *Tellus* **17** 321
- [4] Nese J M 1989 *Physica D* **35** 237
- [5] Mukougawa H et al 1991 *J. Atmos. Sci.* **48** 1231
- [6] Kazantsev E 1999 *Appl. Math. Comput.* **104** 217
- [7] Ziemann C et al 2000 *Phys. Lett. A* **4** 237
- [8] Yoden S and Nomura M 1993 *J. Atmos. Sci.* **50** 1531
- [9] Lacarra J F and Talagrand O 1988 *Tellus A* **40** 81
- [10] Mu M et al 2003 *Nonlinear Process. Geophys.* **10** 493
- [11] Li J P, Ding R Q and Chen B H 2006 *Review and Prospect on the Predictability Study of the Atmosphere* (Beijing: China Meteorology Press) p 96
- [12] Ding R Q and Li J P 2007 *Phys. Lett. A* **364** 396
- [13] Chen B H et al 2006 *Sci. Chin. D* **49** 1111
- [14] Henon M 1976 *Comm. Math. Phys.* **50** 69
- [15] Bergen R E and Harnack R P 1982 *Mon. Wea. Rev.* **110** 1083
- [16] Toth Z 1989 *J. Climat.* **2** 594
- [17] Kalnay E and Dalcher A 1987 *Mon. Wea. Rev.* **115** 349
- [18] Legras B and Ghil M 1985 *J. Atmos. Sci.* **42** 433